IS-m 920

Practical analysis of materials with depth varying compositions using FT-IR photoacoustic spectroscopy (PAS)

John F. McClelland, Roger W. Jones, and Siquan Luo

Ames Laboratory, Iowa State University, Ames, Iowa 50011-3020; and MTEC Photoacoustics, Inc., Ames, Iowa 50014

(Received

FT-IR photoacoustic spectroscopy (PAS) is discussed as a nondestructive method to probe the molecular composition of materials versus depth on the basis of the analysis of layers of experimentally controllable thickness, which are measured from the sample surface to depths of some tens of micrometers, depending on optical and thermal properties. Computational methods are described to process photoacoustic amplitude and phase spectra for both semi-quantitative and quantitative depth analyses. These methods are demonstrated on layered and gradient samples.

PACS numbers: 81.70.Cv, 81.70.Jb, 82.80.Gk, 82.80.Kq

This work was funded in part by the Iowa State University of Science and Technology under Contract No. W-7405-ENG-82 with the U.S. Department of Energy.

I. INTRODUCTION

Materials with depth-varying molecular composition play an important role in both manmade and natural products. For example, coating systems, multilayer polymer packaging films, and medical devices, as well as numerous biological materials, utilize various gradient or layered structures to achieve desired functions. Spectroscopic molecular analysis probes are needed to characterize such materials nondestructively with a surface-to-bulk probe-depth range of tens of micrometers and a depth resolution varying from fractions of a micrometer to several micrometers. Capability to analyze both planar and non-planar samples is desirable.

Infrared spectroscopic measurements based on reflection and transmission do not offer a nondestructive way to vary probe depth over the depth range of interest. Confocal Raman microscopy allows detection of Raman emission from small volume elements below the sample surface. Its capabilities and limitations, however, are not the subject of this paper, which focuses on the use of FT-IR photoacoustic spectroscopy (PAS) for studying layered and gradient samples.

FT-IR PAS is ideally suited for depth analysis because of the role of thermal waves in photoacoustic signal generation. Their short and externally controllable decay distances within the sample determine the layer thickness below the sample surface from which the signal is detected. The thickness range extends from sub-micrometer to tens of micrometers. Furthermore, the propagation time of thermal waves within the sample gives depth-specific information because signals generated by molecular absorption deep within the sample are delayed in time relative to those produced by absorption closer to the surface.

II. PHOTOACOUSTIC SIGNAL GENERATION CONSIDERATIONS IN DEPTH ANALYSIS

The PAS signal generation sequence starts with the infrared beam of the FT-IR spectrometer being incident on the sample and the non-reflected beam component penetrating into the sample a distance approximately equal to $1/\alpha$, where α is the sample optical absorption coefficient.[1,2] Absorption and thermalization of the light, which is intensity modulated by the interferometer, results in instantaneous temperature oscillations within the sample. The instantaneous oscillation amplitudes, excited at a particular radiation wavenumber, decay exponentially with depth into the sample according to the value of α at that wavenumber. Each layer of the sample that absorbs light and experiences temperature oscillations generates thermal waves with a decay coefficient given by $a_s = (\pi f/D)^{1/2}$, where f is the experimentally controllable light-intensity modulation frequency, and D is the sample thermal diffusivity.[1] These absorption-generated thermal waves propagate back in part to the incident beam surface and cause the gas atmosphere in contact with the surface also to oscillate in temperature. This results

in pressure oscillations in the small-volume sample chamber of the photoacoustic detector, which are detected by a sensitive microphone as the photoacoustic signal. The amplitude of the pressure oscillations increases with α, thus allowing the absorbance spectrum of the sample to be measured.

In the range where α is less than or approximately equal to a_s, the probe depth is approximately equal to the thermal diffusion length, $L = 1/a_s = (D/\pi f)^{1/2}$, because thermal waves generated deeper than L make a minor contribution to the temperature oscillations in the gas. L can be adjusted by changing the beam intensity modulation frequency, f, over a wide range. If α increases to values larger than a_s, the probe depth becomes limited by the decay of light rather than by the decay of thermal waves within the sample.

Table I gives thermal-wave propagation parameters[2] for a range of frequencies including: L; VT (the distance that a thermal wave travels in one oscillation period, $T = 1/f$, with a velocity, $V = (4\pi Df)^{1/2}$); and t/θ_t, which represents the number of micrometers that a thermal wave travels in the sample per degree of phase delay. For instance, at 100 Hz it can be seen from Table I that a thermal wave experiences a 10° phase delay crossing a 3.1 μm thick layer.

The decay of thermal waves within the sample and their role in phase delay allow probing of layers of variable thickness below the sample surface. Variations in layered and gradient compositions are revealed as the probe depth is increased by reducing the modulation frequency. A number of factors must be considered, however, in interpreting photoacoustic spectra measured at different frequencies and phase delays. In rapid-scan FT-IR measurements, the interferometer optical-path-difference velocity, v, determines L according to the formula $L = (D/\pi\nu v)^{1/2}$, where ν is the wavenumber of a particular point in the spectrum. Consequently, in rapid-scan measurements, L varies across the spectrum. Alternatively, if step-scan FT-IR

measurements are made, the modulation frequency is determined by a phase modulation, which occurs when a small-amplitude oscillation occurs in the position of one of the interferometer mirrors. This mode of operation produces a constant value of L across the spectrum and also offers easy access to the phase of the PAS signal, in addition to its amplitude.

The variable probe depth nature of PAS results in two factors that must be accounted for. The first is that spectra have increased saturation (truncation of strong bands) as L values are increased, just as transmission spectra do when the sample path length is increased. The spectral changes associated with increasing saturation can be difficult to distinguish from spectral changes caused by compositional changes observed as L increases. When sample conditions allow it, the simplest way to deal with saturation effects is to scale all of the depth-varying spectra so that the intensities are equal for a weak band associated with a major component that is known to have little depth variation. This scaling allows spectral changes from depth varying components to be observed semi-quantitatively when spectral overlap is minimal and the absorbance bands of interest are weak. In many practical applications, such is not the case, or a more quantitative analysis is required. A general quantitative method to compensate for increasing saturation is described in the next section.

The second factor to be accounted for is that spectra measured at a given L value (or range of L values in a rapid-scan measurement) are representative of an average concentration (weighted by the exponential decay coefficients α and a_s) within the layer. In many instances, however, one needs to know concentration as a function of depth. Calculating concentration profiles from a group of PAS spectra taken at different L values is complicated by the general problem commonly encountered in inverse-theory problems in which solutions tend to be unstable and may lead to large prediction errors. In the next section, an approach is described in

which a functional form, based on supplemental information, is used to stabilize the profile calculation.

The phase component of the photoacoustic signal also has important compositional information related to depth. The phase delay for a very strong absorbance peak approaches a phase shift of 90°, whereas a very weak absorbance has approximately a 135° phase shift relative to the excitation waveform for a homogeneous sample.[1] Non-homogeneous samples can have both smaller or larger phase shifts than is the case for homogeneous samples, depending on the thermal, optical, and dimensional properties of the sample and the modulation frequency. In the case of layered samples, all of the phase delays associated with the absorbance bands of a particular layer are clustered within the same range of phase-shift angles with the first layer's cluster having the least delay, the next deeper layer cluster the next-to-the-least delay, and so forth.[3] This sequencing of layer clusters allows the layer order of multi-layer films to be determined, as will be shown in a later section.

Since the PAS signal has amplitude and phase components, it is a vector quantity, which in the case of a two-layer structure allows the separation of the superimposed signals from the two layers by looking at orthogonal components of the signal. Another useful procedure is to use the amplitude and phase to calculate a linearized photoacoustic spectrum that has less saturation than a conventional magnitude spectrum. This procedure is described in the next section, and an application example is presented in the following section of the use of linearization.

III. SIGNAL PROCESSING FOR DEPTH ANALYSIS

A. Saturation equalization

Most data-processing methods aimed at depth analysis make use of phase information, but the earliest method was the direct comparison of spectra taken at different scanning speeds or modulation frequencies, which, as previously discussed, results in different thermal diffusion lengths, L, and so different effective probe depths. An example of this is presented in Polymer Additives below. The difficulty with this is the increase in spectral saturation that accompanies lowering the scan speed or frequency. Fortunately, it is possible to remove most of the saturation differences between low and high scanning-speed spectra so that they may be more readily compared. A low-speed (or frequency) spectrum can be converted into a spectrum with the amount of saturation of a high-speed (or frequency) spectrum using the theory for photoacoustic signal generation in homogeneous samples.[1,4] This removes the saturation differences between spectra at different speeds or frequencies while retaining any differences related to sample structure. The idea is to use a spectrum peak, G, that is known to arise from a homogeneous component in the sample as a guide for reducing the amount of saturation in the low speed (or frequency) spectrum.[5] For a homogeneous component and normalized spectra, the ratio, $\mathbf{R}_n$, of the signal at a given wavenumber in a high-speed spectrum, $\mathbf{Q}_h$, to that in a low-speed spectrum, $\mathbf{Q}_l$, depends only on the ratio of the two speeds (high/low), N, and how much saturation is present. The guide peak, G, is used to determine the amount of saturation. The maximum photoacoustic signal, $\mathbf{Q}_{max}$, occurs at full saturation, so a spectrum can be rescaled so that a value of 1 equals total saturation by dividing each point in the spectrum by $\mathbf{Q}_{max}$. This scaled signal, $\mathbf{Q}_{sc}$, can then be related to $\mathbf{R}_n$:[5]

$$\mathbf{R}_n = \frac{1}{N^{1/2} + \mathbf{Q}_{sc}(1 - N^{1/2})} \qquad (1)$$

$$\mathbf{Q}_{sc} = \frac{\mathbf{Q}}{\mathbf{Q}_{max}} = \frac{N^{1/2}\mathbf{R}_n - 1}{\mathbf{R}_n(N^{1/2} - 1)} \tag{2}$$

Eqs. (1) and (2) involve the vectors $\mathbf{Q}_{sc}$ and $\mathbf{R}_n$, which include phase, but they can be converted to analogous, but substantially more complicated, equations for the signal magnitudes, Q_{sc} and R_n. These equations are given in Reference 5.

G guides the conversion of a high-saturation, low-speed spectrum into a low-saturation, high-speed-equivalent spectrum that retains the probe depth (thermal diffusion length) of the low speed. First, high- and low-speed spectra are acquired from a sample. The ratio R_n is determined for *G* from its magnitudes in the observed high-speed and low-speed spectra, then the value of Q_{sc} for *G* is calculated from the magnitude analog of Eq. (1). This establishes the Q_{sc} values for the whole spectrum because it is just a linear scaling. Substituting the Q_{sc} values into the analog of Eq. (2) then gives R_n values for the whole spectrum. Multiplying the data-points in the low-speed spectrum by their R_n values results in the high-speed-equivalent spectrum.

Fig. 1 shows the conversion process applied to two different samples. Spectra of a homogeneous polypropylene sample are at the bottom, and above them are spectra of polypropylene containing an additive that has been diffused in from the sample surface, so it is concentrated near the surface. In each group, the dashed and dash-double-dot spectra were taken at scanning speeds of 100 Hz and 5 kHz (laser-fringe speeds, equivalent to 0.0063 and 0.032 cm/s OPD velocities). In both sets, the solid-line spectrum is the 100 Hz spectrum after conversion to 5 kHz equivalence. For the pure polypropylene, the true 5 kHz spectrum and the converted spectrum are close matches, as they should be if the saturation levels have been equalized. For the sample containing the additive, the heights of the polypropylene bands match in the 5 kHz and converted spectra but the additional bands from the additive do not; they are distinctly stronger in the true 5 kHz spectrum, indicating

that the concentration of the additive drops off with sample depth. A quantitative example of applying this saturation-equalization method is described in Polymer Weathering below.

B. Phase calculation

With the advent of phase-modulation (commonly called step-scan) FT-IR spectrometers, using phase for photoacoustic depth-profiling became more common because phase modulation provides ready access to both the magnitude and phase of the photoacoustic signal vector. Fig. 2 shows the relationship among the various vectors and measurements involved. The photoacoustic signal vector, **Q**, at a given wavenumber has a magnitude, M, and an observed phase, θ. This observed phase is not the same as the true photoacoustic phase because it also contains contributions from the spectrometer and depends on where the spectrometer defines 0° to be. Many spectrometers allow either the sample itself or some other reference material to be used as the phase reference. Zero degrees will then be set equal to the phase of that reference. If the sample itself is used, then $\theta = 0°$, and no useful phase information is retained. More usefully, the reference can be a thermally thick sample that absorbs all infrared radiation right at the surface. The phase for such a reference will be as fast as is possible for thermally thick, homogenous material, so all thermally thick, homogenous samples will lag behind it by between 0° and 45°.[1,4] Layered samples can have phases outside this range, however. We have found glassy carbon to be a good choice for such a reference.[6]

When phase-modulation spectra are acquired, the spectrometer typically produces two orthogonal component spectra, which have magnitudes M_0 and M_{90} at a given wavenumber and are

the projections of **Q** onto the 0° and 90° axes, as shown in Fig. 2. The magnitude and phase of the photoacoustic signal are then typically calculated this way:

$$M = (M_0^2 + M_{90}^2)^{1/2} \tag{3}$$

$$\theta = \tan^{-1}\left(\frac{M_{90}}{M_0}\right) \tag{4}$$

It should be kept in mind that the usual Fourier transform process usually causes M_0 and M_{90} to be positive valued at all wavenumbers, and this forces θ to be between 0° and 90° when Eq. (4) is used. The actual value of θ may be outside this range for layered and other structured samples. Using interferograms to determine phase can mitigate this problem somewhat because it allows θ to have a 180° range.[2,7]

In the analysis of layered samples, it is often advantageous to determine the sample spectrum at a specific detection phase angle, in the manner of a lock-in amplifier. For example, proper choice of the detection angle can isolate the spectrum of one layer in a two-layer sample. The spectrum at a specific angle, ϕ, is a projection of **Q** onto the ϕ axis, as shown in Fig. 2, and is related in the following manner to the other quantities discussed:

$$\begin{aligned} M_\phi &= M\cos(\phi - \theta) \\ &= M_0\cos\phi + M_{90}\sin\phi \end{aligned} \tag{5}$$

C. Linearization

The strongest peaks in most FT-IR photoacoustic spectra show some saturation effects (i.e., a sub-linear dependence of signal magnitude on the absorption coefficient). The onset of saturation

for homogeneous samples is moderately low, occurring roughly when the absorption coefficient, α, equals $1/(10L)$, where L is the thermal diffusion length. Increasing the scanning speed or modulation frequency will lower L and reduce saturation, but often this cannot be done. Saturation increases only gradually with increasing α, however, so full saturation does not occur until about $\alpha = 20/L$, and useful spectra can be acquired out to near this limit. Fortunately, the range over which partial saturation occurs is also the range where the phase of the photoacoustic signal is most sensitive to the absorption coefficient,[8] so phase can be used to correct the magnitude spectrum for saturation; that is, to *linearize* it. The linearized spectrum, q_{lin}, can be calculated from the real and imaginary component spectra of the sample and a phase reference:[9]

$$q_{lin} = \frac{q_s^2}{R_s I_r - I_s R_r} \tag{6}$$

where q_s is the observed (partly saturated) sample spectrum, R_s and I_s are the real and imaginary components of the sample spectrum, and R_r and I_r are the real and imaginary components of the phase-reference spectrum. The phase reference, like that for phase-modulation spectra, must absorb the spectrometer beam right at its surface, so that it produces the earliest possible photoacoustic phase for a thick, homogeneous sample. Again, glassy carbon has proven to be a good choice.[6]

What relevance does spectrum linearization have to depth-variation analysis? The greater the amount of saturation in a peak, the earlier its phase, so in the linearization process the earlier the phase is for a peak, the greater its observed magnitude is increased to restore linearity. For a non-homogeneous sample, the spectrum bands arising from any species concentrated at or near the sample surface will have particularly early phases, so when the spectrum is linearized, these surface-species bands enlarge disproportionately and are easily picked out. An example of this is discussed below in Linearization for High Surface Specificity.

IV. APPLICATION EXAMPLES

A. Polymer additives

Additives are often mixed into polymers to provide improved surface and bulk properties for specific applications. Surface additives are engineered to migrate to the surface and provide properties such as lubrication for mold release or static-charge reduction, whereas bulk additives often stabilize polymers to withstand ultraviolet radiation or thermal stress. Fig. 3 shows variable probe-depth spectra of polyethylene polymer pellets containing both surface segregating and bulk additives. These spectra where scaled so that the polyethylene band at 1370 cm^{-1} is of equal height in all spectra to reduce saturation effects for the weaker bands. This scaling obviously is ineffective for the strong polyethylene band at 2900 cm^{-1}, as well as the polyethylene bands at 1440 cm^{-1} and 720 cm^{-1}, all of which increase in height with decreasing L (increasing f) as the level of saturation decreases, despite the fact that their concentration is essentially constant with depth. On the other hand, the scaling allows the behavior of weak bands as a function of depth to be readily observed. The surface additive band at 1650 cm^{-1} is observed to grow with decreasing L, indicating higher concentration at the surface, while the bulk additive band at 1020 cm^{-1} remains constant, indicating a uniform concentration to a depth of approximately 40 μm.

B. Polymer weathering

The scaling just described, while useful in some cases, is not sufficient as a general method to compensate for saturation differences as a function of L. A general method to compensate for saturation differences in spectra, as described in the last section, was applied to weathering studies of PET polymers containing different concentrations of an ultraviolet stabilizer. Fig. 4 shows saturation-compensated peak-height points of the 3271 cm^{-1} hydroxyl absorbance band plotted as a function of L for weathered samples having 0%, 1%, and 2% ultraviolet stabilizer concentrations and for an unweathered sample. The curves in Fig. 4 are least-squares fits to the data points of the photoacoustic signal equation:

$$S = C\left(c_0 + \sum_{i=1}^{n} \frac{c_i}{1-d_i}\right) \tag{7}$$

with n = 2, where C, c_0, c_i, and d_i are fitting constants. Eq. 7 is the form expected for gradients consisting of a sum of exponentials:[5]

$$\alpha(x) = c_0 + \sum_{i=1}^{n} c_i e^{d_i x} \tag{8}$$

where x is depth. Once the fitting constants are obtained from the least-squares fits to the data in Fig. 4, absorption coefficient versus sample-depth curves can be calculated from Eq. 8, as shown in Fig. 5. The points shown in Fig. 5 were obtained from lapping measurements and are in close agreement with the calculated curves, confirming the photoacoustic analysis.

C. Linearization for high surface specificity

Linearized photoacoustic spectra, as discussed in the last section, accentuate the photoacoustic signal components generated closest to the surface and result in spectra that are similar to what would be measured if the modulation frequency were increased by approximately a factor of 10. Fig. 6 illustrates this for the same polyethylene sample containing additives that was discussed earlier. Comparison of Figs. 3 and 6 shows that the surface-segregating-additive and the bulk-additive absorbance bands behave the same as the sampling-depth changes in the two figures. In the case of Fig. 6, the standard magnitude spectrum and the linearized spectrum were both calculated from a single, simultaneous acquisition of the amplitude and phase spectra.

D. Multi-layer analysis using phase

Phase analysis is applicable to both planar and non-planar samples, including microsamples such as single fibers, which is illustrated in Fig. 7. The top panel of Fig. 7 shows the spectrum of a single nylon-coated PET fiber and reference spectra for nylon (above) and PET (below). The magnitudes of a series of nylon and PET absorbance bands are plotted as a function of detection angle in the bottom panel. These bands are all of approximately the same magnitude and would be expected to have their minima close together for a homogeneous sample. However, as discussed in the second section, phase-angle minima for each layer of a layered sample are expected to cluster together, with the first-layer cluster having the smallest phase angles and deeper layers having progressively larger angles. This prediction is well illustrated in this example of a two component system.

V. CONCLUSIONS

This paper has reviewed the use of FT-IR photoacoustic spectroscopy as a means to nondestructively analyze the molecular composition of samples as a function of depth. The technique is shown to be applicable to both planar and non-planar samples in macro and micro sizes. The ability of the technique to probe from the sample surface to experimentally controlled depths is due to the decay and finite-velocity properties of thermal waves, which are generated when the sample absorbs infrared radiation from the spectrometer.

A computational method was discussed to compensate for increases in spectral saturation (strong absorbance band truncation), which occur with increasing probe depth, so that spectral changes due to compositional changes with depth could be observed. A second computational method that provides higher surface specificity was described, which utilizes photoacoustic signal amplitude and phase data to linearize spectra and achieve the equivalent of a factor of ten higher modulation frequency. A third method was outlined for plotting photoacoustic spectra as a function of phase detection angle, which allows phase shifts due, for instance, to thermal wave propagation across layers to be observed for analytical purposes.

Application examples were presented using: spectra measured at different frequencies and linearization to observe the depth distribution of additives in polyethylene; saturation compensation to determine the depth distribution of weathering-induced hydroxyl species in PET; and phase analysis to differentiate between the coating and fiber-core polymers of a single micro-fiber.

ACKNOWLEDGMENT

The authors wish to thank Digilab for technical support and for loan of an FT-IR spectrometer used for some of the work reported here. A portion of the work reported here was performed under CRADA No. AL-C-2000-01, jointly funded by the Office of Science of the U. S. Department of Energy, Ford Motor Company, Minnesota Mining and Manufacturing Company, Sherwin-Williams Company, and MTEC Photoacoustics, Inc. This work was funded in part by the Iowa State University of Science and Technology under Contract No. W-7405-ENG-82 with the U.S. Department of Energy.

REFERENCES

[1] A. Rosencwaig and A. Gersho, J. Appl. Phys. **47**, 64 (1976).

[2] J. F. McClelland, R. W. Jones, and S. J. Bajic, *Handbook of Vibrational Spectroscopy*, edited by J. M. Chalmers and P. R. Griffiths (Wiley, Chichester, UK, 2002), Vol. 2, p. 1231.

[3] E. Y. Jiang, R. A. Palmer, and J. L. Chao, J. Appl. Phys. **78**, 460 (1995).

[4] F. A. McDonald and G. C. Wetsel, Jr., J. Appl. Phys. **49**, 2313 (1978).

[5] R. W. Jones and J. F. McClelland, Appl. Spectrosc. **56**, 409 (2002).

[6] R. W. Jones and J. F. McClelland, Appl. Spectrosc. **55**, 1360 (2001).

[7] R. W. Jones and J. F. McClelland, Appl. Spectrosc. **50**, 1258 (1996).

[8] Y. C. Teng and B. S. H. Royce, J. Opt. Soc. Am. **70**, 557 (1980).

[9] R. O. Carter III, Appl. Spectrosc. **46**, 219 (1992).

Table I. Thermal Wave Propagation Parameters for Different Modulation Frequencies (for $D = 10^{-3}$ cm^2/s)

f(Hz)	L (μm)	VT (μm)	t/θ_t (μm/degree)
1	178	1120	3.1
10	56.4	354	0.98
50	25.2	159	0.44
100	17.8	112	0.31
400	8.92	56.0	0.16
1000	5.64	35.4	0.10
10000	1.78	11.2	0.031

FIGURE CAPTIONS

FIG. 1. Spectra of polypropylene with and without a near-surface additive. In each case, the low-speed (100 Hz) spectrum is transformed so as to have the same amount of saturation as the high-speed (5 kHz) spectrum. In the homogeneous sample, the converted spectrum matches the high speed spectrum. In the other, the gradient of the additive makes the additive peaks smaller in the converted spectrum than in the high-speed spectrum.

FIG. 2. Relationships of the photoacoustic signal vector, **Q**, with its magnitude, M, and phase, θ, to the orthogonal component magnitudes, M_0 and M_{90}, and the magnitude, M_ϕ, observed at a detection angle of ϕ.

FIG. 3. Spectra taken at the three marked scanning speeds of polyethylene pellets containing two additives, one uniformly dispersed and the other concentrated at the surface. Increasing speed both reduces saturation on the larger polyethylene peaks, causing them to grow, and reduces the photoacoustic probe depth, causing the surface-additive peak at 1650 cm^{-1} to grow as well. The uniform-additive peak at 1020 cm^{-1}, however, remains unchanged. The spectra have been scaled so that the small 1370 cm^{-1} peak is of constant size.

FIG. 4. The markers are observed peak heights for a hydroxyl band at 3271 cm^{-1} in spectra of weathered PET samples containing various amounts of an ultraviolet-protection additive. The spectra were taken at various scanning speeds and then saturation equalized. The equalization process reveals the intrinsic drop off with thermal diffusion length of the hydroxyl peaks, which would normally be masked by a saturation-induced increase in overall signal strength. The lines are least-squares fits to the data, assuming the hydroxyl concentration profiles are double exponentials.

FIG. 5. The lines are depth profiles for hydroxyl in weathered PET derived from the fits in Fig. 4. The markers are confirming measurements of peak heights at a single, high scanning speed made as the samples were lapped off to reveal successive depths within the original, intact material. All four depth profiles have been scaled by the same amount to match the ordinate scale of the lapping measurements.

FIG. 6. The effect of linearization on the spectrum of the same polyethylene-with-additives sample used for Fig. 3. Linearization acts like increasing the scanning speed by reducing saturation in large peaks and emphasizing bands of near-surface species, such as the 1650 cm^{-1} band of the surface-concentrating additive.

FIG. 7. Upper panel: Spectrum of a single nylon-coated PET fiber compared to reference spectra of nylon and PET. Lower panel: Magnitudes of the bands marked in the upper panel shown as a function of detection angle. The PET bands all clearly peak at later (higher) angles because the energy deposited in the PET must transit through the nylon coating before generating a photoacoustic signal.

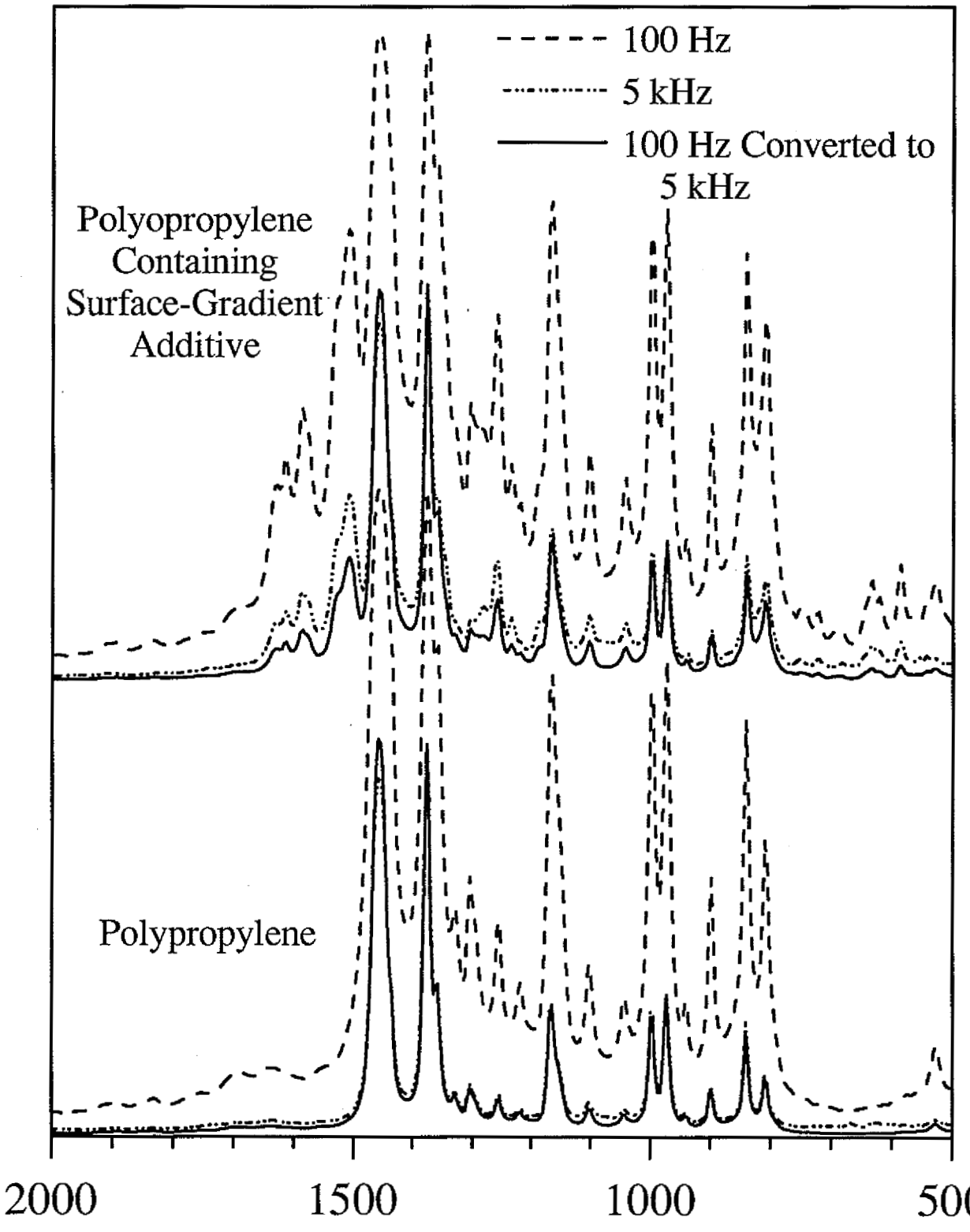
100 Hz
5 kHz
100 Hz Converted to 5 kHz
Polyopropylene Containing Surface-Gradient Additive
Polypropylene
2000
1500
1000
500
Wavenumber (cm-1)

Figure 1

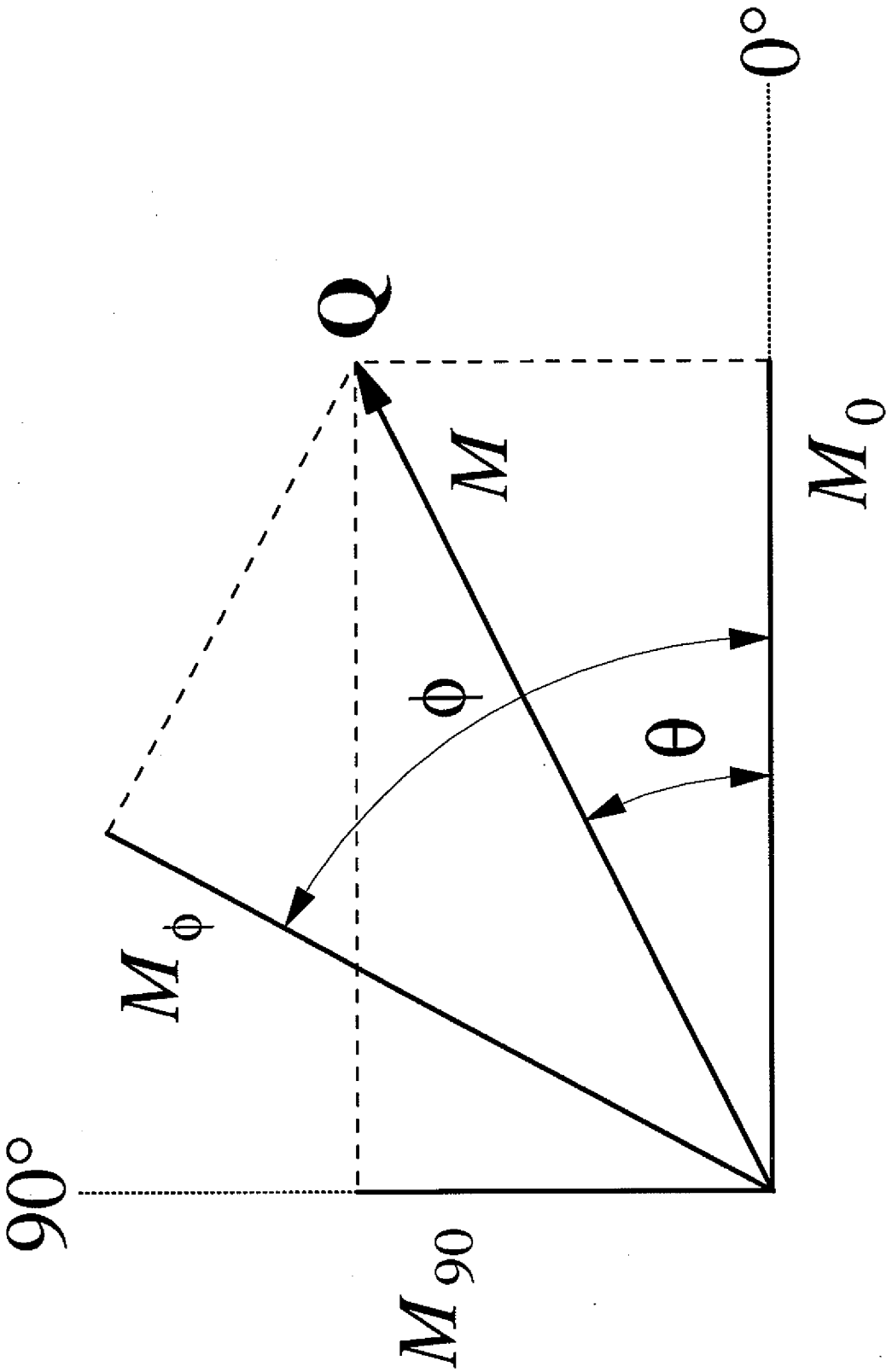

Figure 2

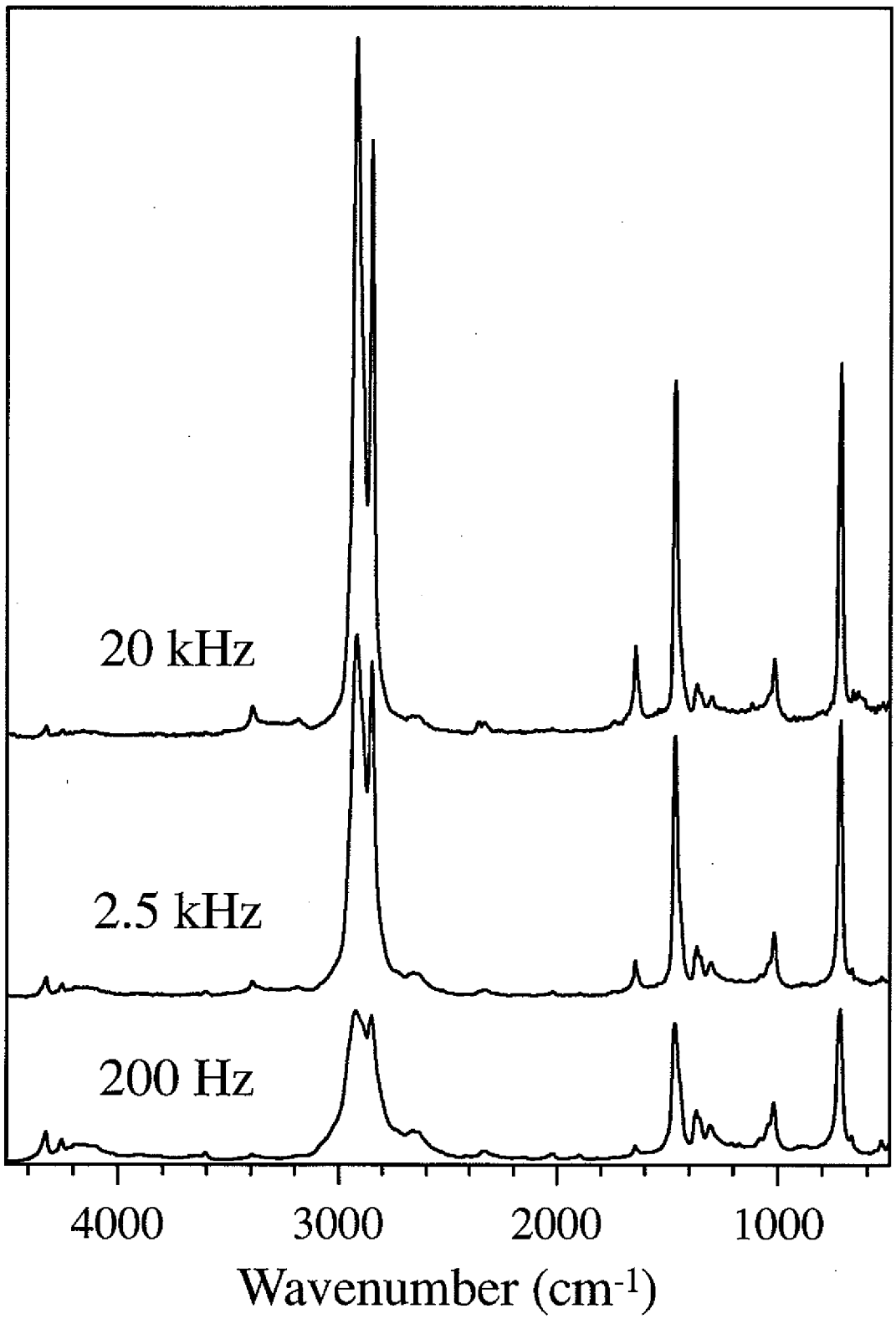

Figure 3

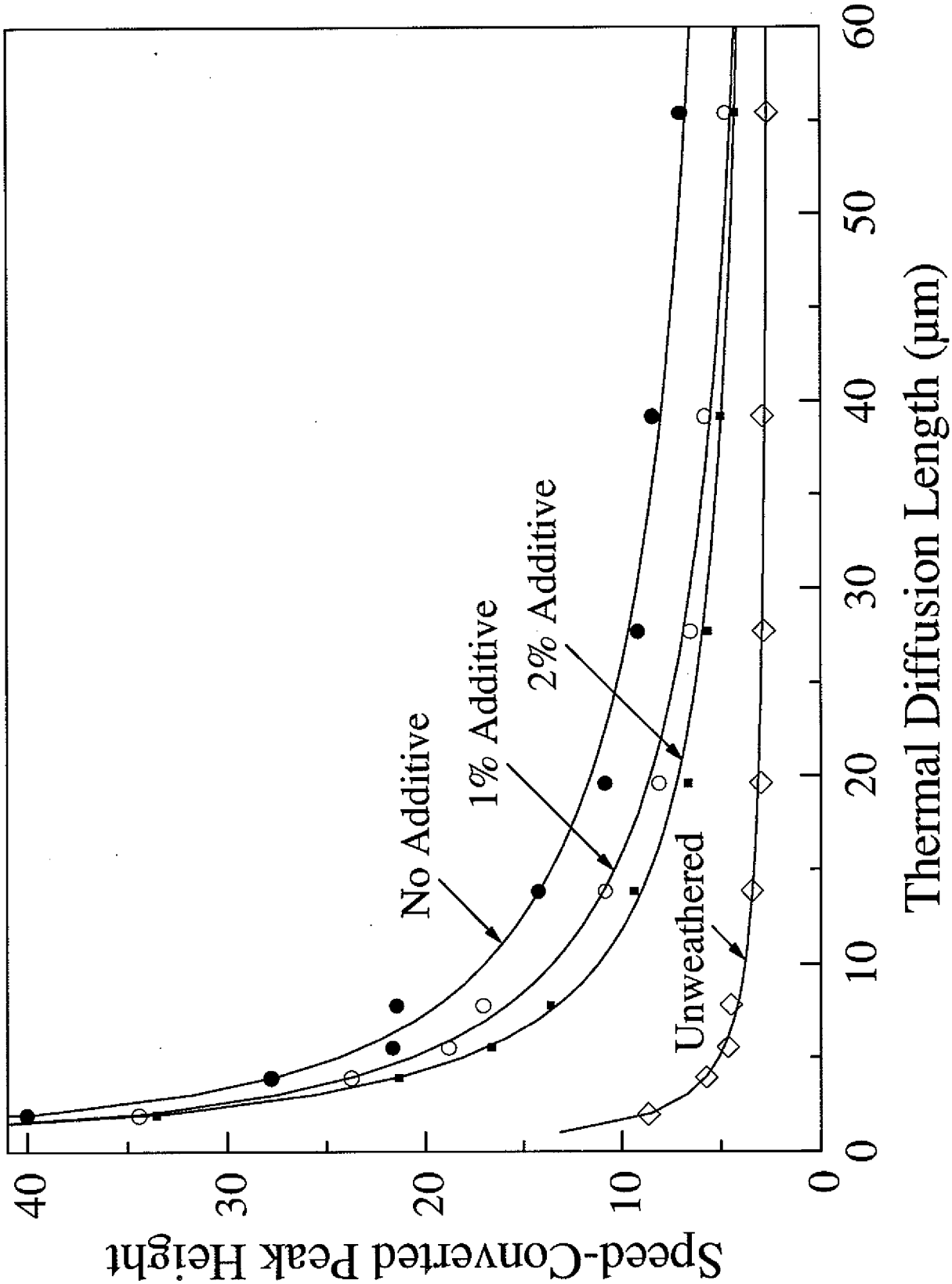
Speed-Converted Peak Height
Thermal Diffusion Length (μm)
0
10
20
30
40
50
60
No Additive
1% Additive
2% Additive
Unweathered

Figure 4

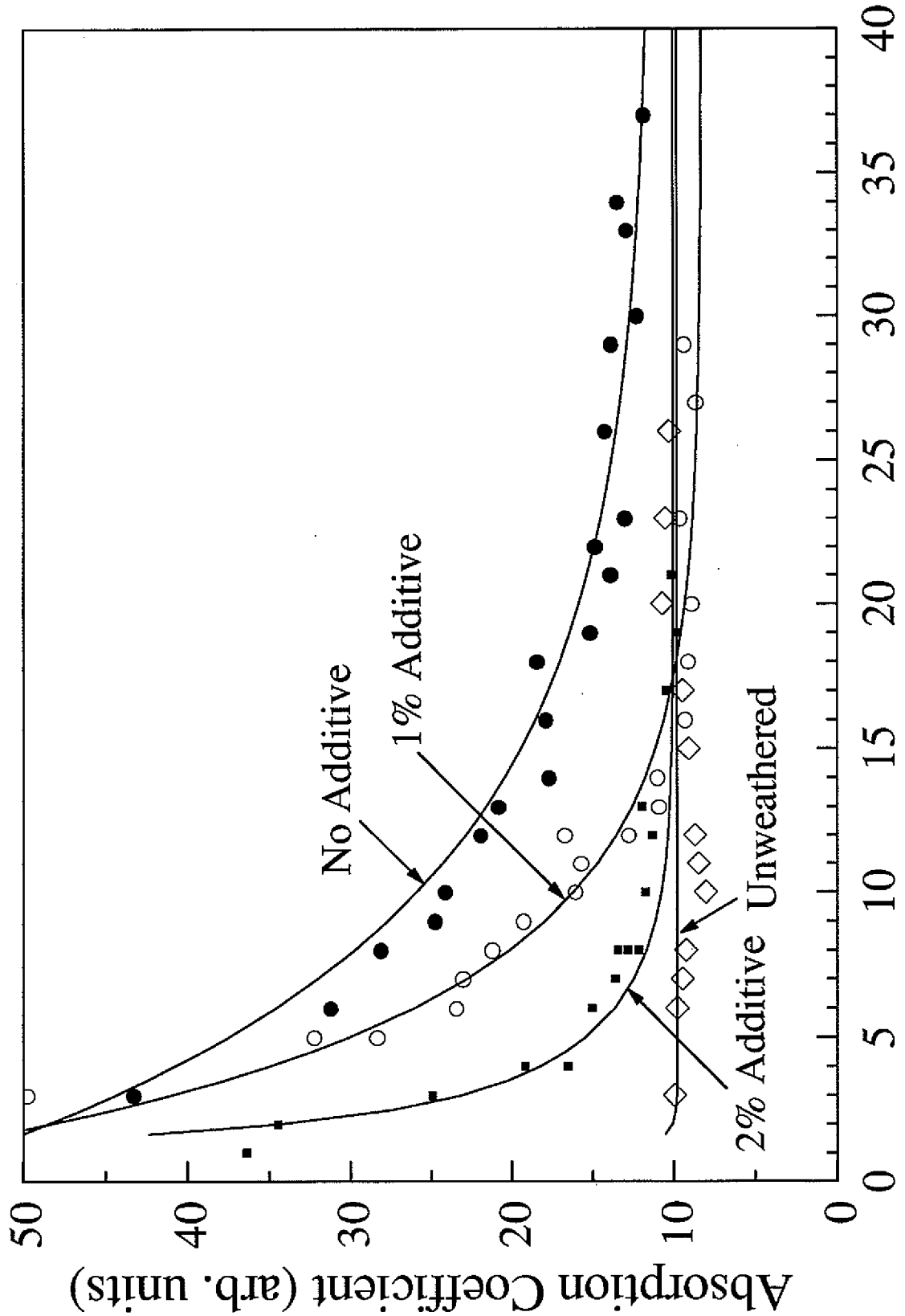
Absorption Coefficient (arb. units)
Sample Depth (μm)
No Additive
1% Additive
2% Additive
Unweathered
0
10
20
30
40
50
0
5
10
15
20
25
30
35
40

Figure 5

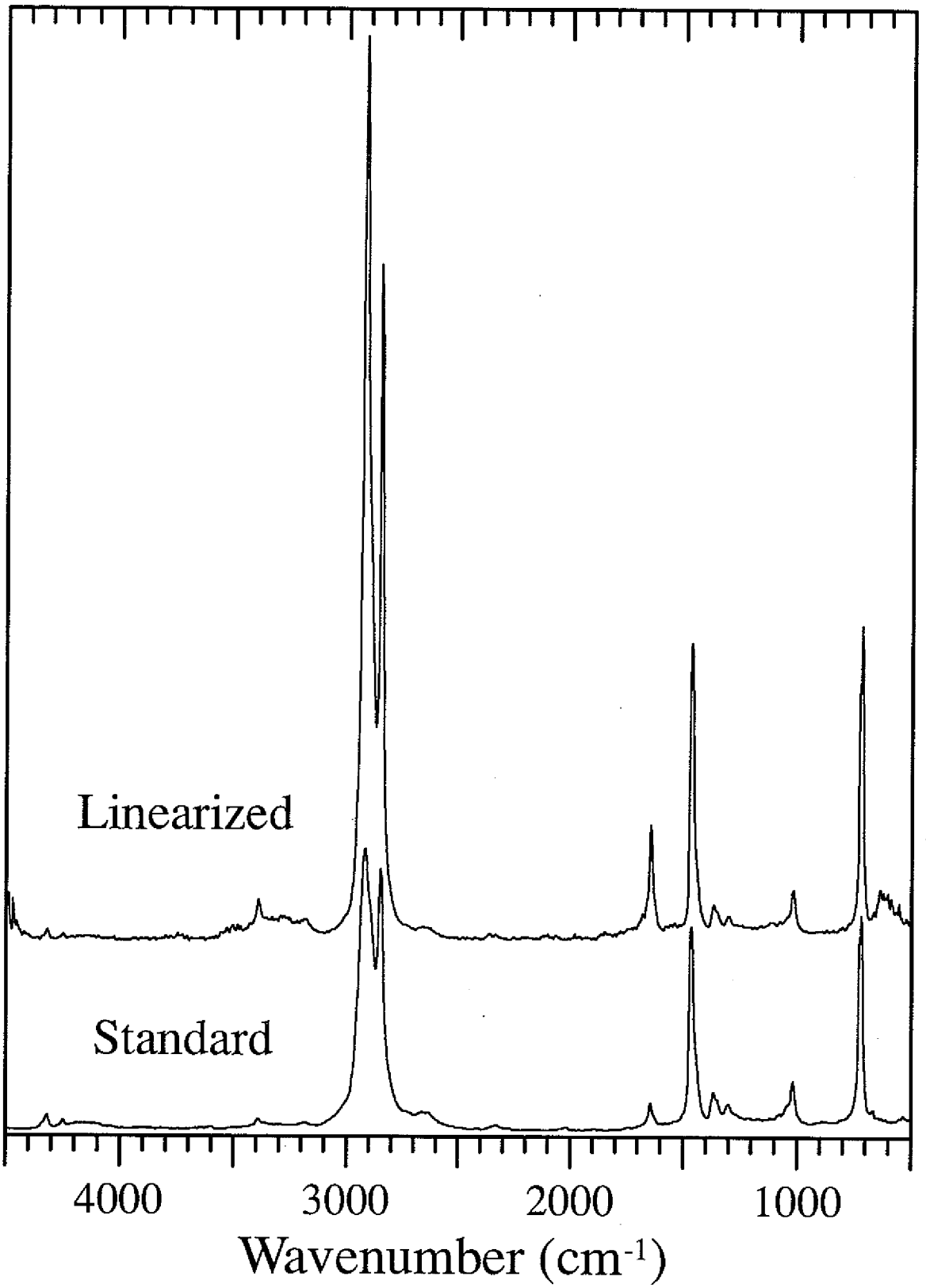

Figure 6

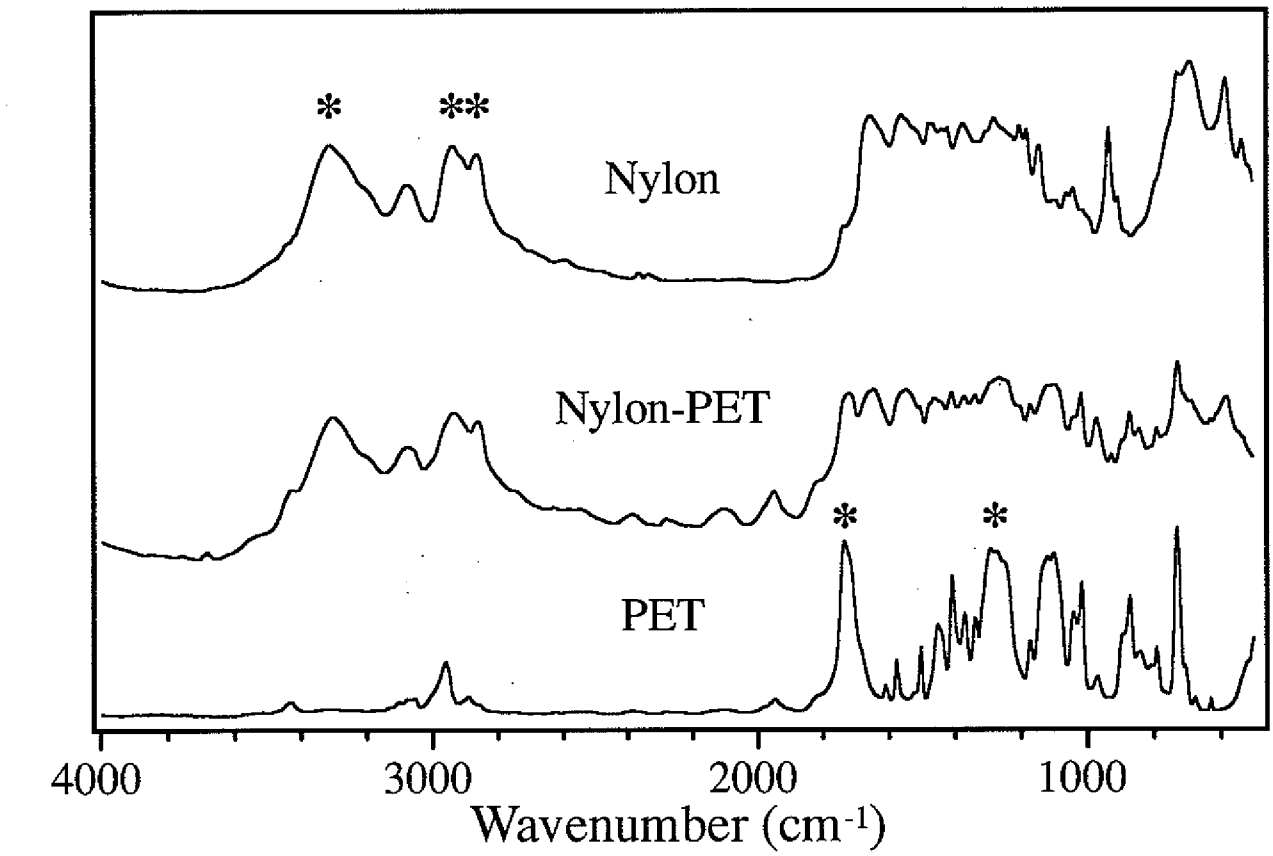
*
**
Nylon
Nylon-PET
*
*
PET
4000
3000
2000
1000
Wavenumber (cm-1)

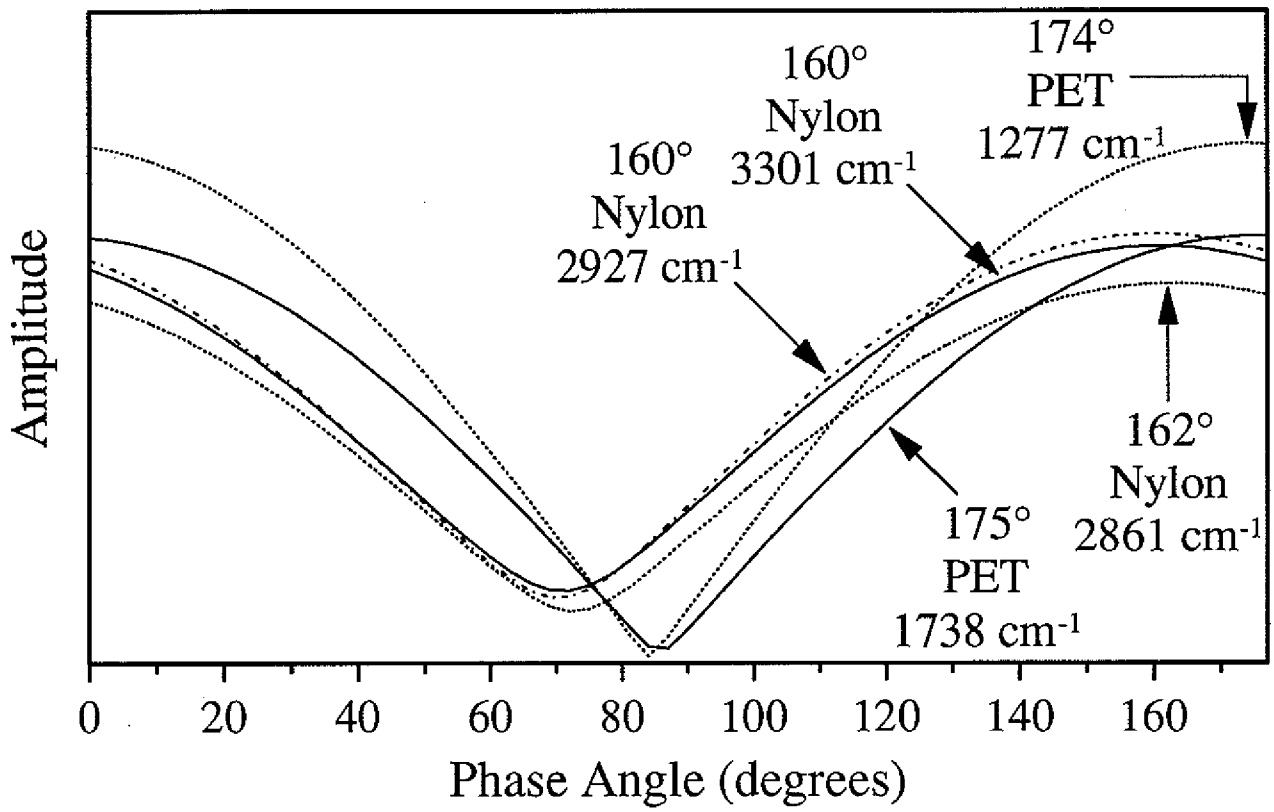
160°
Nylon
2927 cm-1
160°
Nylon
3301 cm-1
174°
PET
1277 cm-1
162°
Nylon
2861 cm-1
175°
PET
1738 cm-1
Amplitude
0
20
40
60
80
100
120
140
160
Phase Angle (degrees)

Figure 7